Spin responses and effective Hamiltonian for the two-dimensional electron gas at the oxide interface LaAlO_{3}/SrTiO_{3}

Jianhui Zhou, Wen-Yu Shan, and Di Xiao

Phys. Rev. B **91**, 241302 — Published 9 June 2015

DOI: 10.1103/PhysRevB.91.241302

Spin responses and effective Hamiltonian for the two dimensional electron gas at oxide interface $LaAlO_3/SrTiO_3$

Jianhui Zhou,* Wen-Yu Shan,† and Di Xiao
Department of Physics, Carnegie Mellon University, Pittsburgh, Pennsylvania 15213, USA

The strong Rashba spin-orbit coupling (SOC) of the two-dimensional electron gas (2DEG) at the oxide interface $LaAlO_3/SrTiO_3$ underlies a variety of exotic physics, but its nature is still under debate. We derive an effective Hamiltonian for the 2DEG at the oxide interface $LaAlO_3/SrTiO_3$ and find a new anisotropic Rashba SOC for the d_{xz} and d_{yz} orbitals. This anisotropic Rashba SOC leads to anisotropic static spin susceptibilities and also distinctive behavior of the spin Hall conductivity. These unique spin responses may be used to determine the nature of the Rashba SOC experimentally and shed new light on the orbital origin of the 2DEG.

PACS numbers: 73.20.–r, 71.70.Ej, 72.25.Mk

The discovery of a high mobility 2DEG at the interface between two band insulators $LaAlO_3$ and $SrTiO_3$ (LAO/STO)[1] has attracted increasing attention[2]. However, the origin of the 2DEG is still under active debate. According to the intrinsic polar catastrophe mechanism, there should be a half electron (per unit cell) transfer from the top surface layer of LAO to the LAO/STO interface. The resulting carrier density at the interface is roughly 3.5×10^{14} cm^{-2}, which mainly comes from the three t_{2g} orbitals of Ti in STO. Several transport experiments, however, estimate that the carrier density is only ten percent of that due to the polar catastrophe mechanism[3–5]. In addition, it has been proposed that electrons in the d_{xy} orbitals, which are confined in the xy-plane, are more likely to become localized at the interface due to the impurities or electron-phonon coupling, while those in the d_{xz} and d_{yz} orbitals are itinerant and contribute to transport[6]. Within this scenario, the localized and itinerant electrons would account for the observed magnetic order[7] and superconductivity[8–11], respectively. It is therefore important to understand the transport properties of the 2DEG. Other mechanisms, such as oxygen vacancies[12,13] and polar distortion[14,15] have also been proposed.

Recent magneto-transport experiments have provided us new insight into the 2DEG at the oxide interface. In particular, a strong and field-tunable Rashba spin-orbit coupling (SOC) was observed[16,17] and was modeled using the standard k-linear form[18], i.e.,

$$H_R = \lambda_R(\boldsymbol{k} \times \boldsymbol{\sigma}) \cdot \hat{z} \, . \tag{1}$$

Based on this k-linear Rashba SOC, theoretical works have predicted a variety of unusual effects such as the Fulde-Ferrell-Larkin-Ovchinikov-type superconductivity coexisting with ferromagnetism[19], spiral magnetic order and skyrmions[20–23], and the spin Hall effect[24]. However, a very recent magneto-conductivity measurement has suggested the possibility of a k-cubed Rashba SOC of the 2DEG at the oxide interface[25,26]. Accordingly, some authors proposed the k-linear Rashba SOC for the d_{xy} orbital[27,28] and k-cubed one for the d_{xz} and d_{yz} orbitals[28]. On the other hand, first-principles calculations combined with the envelope function method have found an anisotropic nonparabolic spin-splitted subband structure for the d_{xz} and d_{yz} orbitals[29], which could not be explained by the standard k-cubed Rashba SOC. Thus, a detailed investigation of the low energy effective model and the nature of the Rashba SOC is highly desirable.

In this paper, we present a detailed derivation of the effective Hamiltonian of the 2DEG at the oxide interface. We find a new anisotropic Rashba SOC of the following form

$$H_R^{\text{ani}} \propto \left(k_x^2 - k_y^2\right)(\boldsymbol{k} \times \boldsymbol{\sigma}) \cdot \hat{z} \tag{2}$$

for the d_{xz} and d_{yz} orbitals, and a standard k-linear Rashba SOC for the d_{xy} orbital. The anisotropy of the Rashba SOC naturally leads to anisotropic spin susceptibilities that have been observed experimentally[10,11]. We also show that this anisotropic Rashba SOC results in different behavior of the spin Hall conductivity (SHC) when compared to the standard k-linear and k-cubed Rashba SOCs. These distinctive spin responses can be used for determining the nature of the Rashba SOC in experiments and shed new light on the orbital origin of the 2DEG at the LAO/STO interface.

We begin by constructing the low-energy effective model of the 2DEG at the LAO/STO interface around the Γ point in the Brillouin zone. The 2DEG is formed from the d-orbitals of the transition-metal Ti. Here we focus on the three t_{2g} orbitals, namely, d_{xy}, d_{xz} and d_{yz}, since the e_g orbitals are pushed up about 2 eV higher than the t_{2g} orbitals by the octahedral crystal field. On the xy-plane, electrons in the d_{xy} orbital can hop along either x or y direction to the d_{xy} orbitals on the neighboring Ti, while electrons in the d_{xz} (d_{yz}) orbital can hop to its neighbor only along the x (y) direction. Thus the corresponding hopping Hamiltonian can be expressed in the following matrix form:

$$H_0 = \begin{pmatrix} h(\boldsymbol{k}) & 0 & 0 \\ 0 & -2t\cos k_x & 0 \\ 0 & 0 & -2t\cos k_y \end{pmatrix}, \tag{3}$$

where $h(\boldsymbol{k}) = -\Delta_E - 2t\left(\cos k_x + \cos k_y\right)$, $t = t_{pd}^2/\Delta_{pd}$ is the effective hopping parameter between nearest neighboring Ti, Δ_{pd} is the splitting between the oxygen p and Ti t_{2g} energy levels, and Δ_E is the difference of the onsite energies between the d_{xy} orbital and the d_{yz}/d_{xz} orbital. Note that since d_{xy} is even, and d_{xz} and d_{yz} are odd under the operation $z \to -z$, hopping between these two sets of orbitals is prohibited in the presence of the mirror symmetry.

To model the effect of the SOC, we introduce the atomic SOC $H_\xi = \xi \boldsymbol{l}\cdot\boldsymbol{\sigma}$ in the basis $\{|d_{xy}\uparrow\rangle, |d_{xy}\downarrow\rangle, |d_{xz}\uparrow\rangle, |d_{xz}\downarrow\rangle, |d_{yz}\uparrow\rangle, |d_{yz}\downarrow\rangle\}$,

$$H_\xi = \xi \begin{pmatrix} 0 & 0 & 0 & -i & 0 & 1 \\ 0 & 0 & -i & 0 & -1 & 0 \\ 0 & i & 0 & 0 & -i & 0 \\ i & 0 & 0 & 0 & 0 & i \\ 0 & -1 & i & 0 & 0 & 0 \\ 1 & 0 & 0 & -i & 0 & 0 \end{pmatrix}, \tag{4}$$

where ξ denotes the strength of the atomic SOC. $\boldsymbol{\sigma}$ refers to the spin degree of freedom, while $\boldsymbol{l}$ is the orbital angular momentum of the electron.

Finally, there is a mirror symmetry breaking at the interface due to the polar displacement of Sr and Ti atoms relative to the oxygen octahedra, which leads to the Rashba SOC. Physically, the mirror symmetry breaking can induce the hopping process from the d_{xz} (d_{yz}) orbital to the d_{xy} orbital via the p_x (p_y) orbital of oxygen. The corresponding Hamiltonian can be written as[27,28]

$$H_\gamma = \gamma \begin{pmatrix} 0 & -2i\sin k_y & -2i\sin k_x \\ 2i\sin k_y & 0 & 0 \\ 2i\sin k_x & 0 & 0 \end{pmatrix} \otimes \sigma_0, \tag{5}$$

where γ refers to the effective hopping amplitude between the d_{xy} orbital and the d_{xz} and d_{yz} orbitals. σ_0 is the 2×2 unit matrix in the real spin space.

The total tight-binding (TB) Hamiltonian including all three parts is given by

$$H_{\mathrm{TB}} = H_0 + H_\xi + H_\gamma\ .$$

There are three pairs of degenerate bands at the Γ point, which are plotted in Fig. 1(a) using the parameters given in Ref. 28. It can be seen that the energy contour of the middle two bands has a strong anisotropy as shown in Fig. 1(b), whereas the lowest two bands are isotropic as shown in Fig. 1(c). Note that the splitting of the lowest two energy bands due to the Rashba SOC is unnoticeable for the given energy.

To derive the effective Hamiltonian, we apply the quasi-degenerate perturbation theory[30]. Up to leading order in the SOC strength ξ, we obtain the effective Hamiltonian for the top pair of bands

$$H_{\mathrm{top}}\left(\boldsymbol{k}\right) = \frac{k^2}{2m_{\mathrm{top}}} - \alpha_{\mathrm{top}}\left(\boldsymbol{k}\times\boldsymbol{\sigma}\right)\cdot\hat{z}, \tag{6}$$

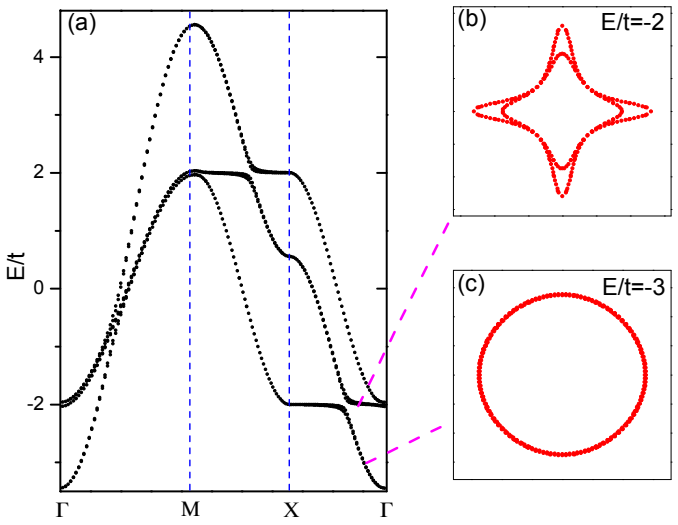

FIG. 1. (Color online) (a) Band structure of TB model describing oxide interface. Energy contours near the Γ point for energies (b) $E/t = -2$ and (c) $E/t = -3$. Parameters are adopted from Ref. 28: $\Delta_E/t = -0.56$, $\xi/t = 0.035$, $\gamma/t = 0.072$.

the middle pair of bands

$$H_{\mathrm{mid}}\left(\boldsymbol{k}\right) = \frac{k^2}{2m_{\mathrm{mid}}} + \alpha_{\mathrm{mid}}\left(k_x^2 - k_y^2\right)\left(\boldsymbol{k}\times\boldsymbol{\sigma}\right)\cdot\hat{z}, \tag{7}$$

and the bottom pair of bands

$$H_{\mathrm{bot}}\left(\boldsymbol{k}\right) = \frac{k^2}{2m_{\mathrm{bot}}} - \alpha_{\mathrm{bot}}\left(\boldsymbol{k}\times\boldsymbol{\sigma}\right)\cdot\hat{z}, \tag{8}$$

where $(m_{\mathrm{top}}, m_{\mathrm{mid}}, m_{\mathrm{bot}})$ and $(\alpha_{\mathrm{top}}, \alpha_{\mathrm{mid}}, \alpha_{\mathrm{bot}})$ are the effective masses and Rashba SOC strengths for the top, middle, and bottom pairs of bands, respectively (all their specific expressions are given in the supplementary materials)[31]. The top pair of bands is a mixture of all three t_{2g} orbitals. The bottom pair mainly comes from the d_{xy} orbital. The middle pair is a hybridization between the d_{xz} orbital and the d_{yz} orbital. It is also clear that the bottom pair of bands has the k-linear Rashba SOC that was proposed by previous works[27,28]. This concentric isotropic Fermi contour of d_{xy} orbital had also been demonstrated at the surface of bare $SrTiO_3$[32]. In the middle pair of bands, the Rashba SOC becomes anisotropic and has a k-cubed energy dispersion[33]. Two recent angle-resolved photoemission experiments had already observed the anisotropic Fermi contour of the d_{xz} orbital and the d_{yz} orbital at a high carrier density[34,35]. Note that the effective Hamiltonian of each pair of bands is constructed with respect to its own bottom edge.

The anisotropic Rashba SOC for the d_{xz} and d_{yz} orbitals in Eq. (7) is our main result. In the rest of this paper, we will study its effects on the static spin susceptibility and the spin Hall conductivity[36,37]. For convenience, we redefine the corresponding effective mass

$m = m_{\rm mid}/\hbar^2$ and Rashba SOC strength $\beta = \alpha_{\rm mid}/\hbar^3$. The effective Hamiltonian for the middle pair can be recast into

$$H_{\rm mid}(\boldsymbol{k}) = \begin{pmatrix} \frac{\hbar^2 k^2}{2m} & -i\beta\hbar^3\left(k_x^2 - k_y^2\right)k_- \\ i\beta\hbar^3\left(k_x^2 - k_y^2\right)k_+ & \frac{\hbar^2 k^2}{2m} \end{pmatrix}, \tag{9}$$

with $k_\pm = k_x \pm ik_y$. Some simple algebra leads to the eigenvalues of $H_{\rm mid}(\boldsymbol{k})$

$$\varepsilon_{\boldsymbol{k}s} = \frac{\hbar^2 k^2}{2m} + s\beta\hbar^3 k^3 \left|\cos 2\theta_{\boldsymbol{k}}\right| \tag{10}$$

and the corresponding eigenvectors

$$\phi_{\boldsymbol{k}s} = \frac{1}{L} e^{i\boldsymbol{k}\cdot\boldsymbol{r}} \eta_{\boldsymbol{k}s}, \tag{11}$$

where the spinor is given by $\eta_{\boldsymbol{k}s} = \left(-is\varsigma_{\boldsymbol{k}} e^{-i\theta_{\boldsymbol{k}}}, 1\right)^T/\sqrt{2}$, $s = \pm 1$ is the chirality index, L^2 is the area of the 2DEG with $\varsigma_{\boldsymbol{k}} = \cos 2\theta_{\boldsymbol{k}}/\left|\cos 2\theta_{\boldsymbol{k}}\right| = \pm 1$, $\theta_{\boldsymbol{k}} = \arctan(k_y/k_x)$. Since our model is only valid around the Γ point, we would like to introduce a momentum cutoff $k_c = 1/3m\hbar\beta$ via the turning point of the energy dispersion $\varepsilon_k = k^2\hbar^2/2m - \beta\hbar^3 k^3$. The corresponding energy of this turning point is given by $\varepsilon_{\rm turn} = 1/54m^3\beta^2$.

In general, the free spin susceptibilities can be written as

$$\chi_{ij}(\boldsymbol{q}) = -k_B T\mu_B^2 \sum_{n,\boldsymbol{k}} {\rm Tr}\left[\sigma_i G(\boldsymbol{k},\omega_n)\sigma_j G(\boldsymbol{k}+\boldsymbol{q},\omega_n)\right], \tag{12}$$

where σ_i are the Pauli matrices with $i = x, y, z$, $G(\boldsymbol{k},\omega_n)$ is the Matsubara Green's function of an electron with momentum $\boldsymbol{k}$ and frequency ω_n, μ_B is the Bohr magneton. After carrying out the standard analytic continuation and frequency summation (more details of the derivation can be found in the Appendix of Ref. 39), we can find the static spin susceptibilities in the limit $\boldsymbol{q} \to 0$,

$$\chi_{zz}^0 = -2\mu_B^2 \sum_{\boldsymbol{k}} \frac{f(\xi_+(\boldsymbol{k})) - f(\xi_-(\boldsymbol{k}))}{\xi_+(\boldsymbol{k}) - \xi_-(\boldsymbol{k})}, \tag{13}$$

$$\chi_{xx}^0 = -\frac{\mu_B^2}{2}\sum_{\boldsymbol{k},\lambda} \frac{\partial f(\xi_\lambda(\boldsymbol{k}))}{\partial\xi_\lambda(\boldsymbol{k})} + \frac{\chi_{zz}^0}{2}, \tag{14}$$

$$\chi_{yy}^0 = \chi_{xx}^0, \tag{15}$$

where $\xi_\lambda(\boldsymbol{k}) = \varepsilon_\lambda(\boldsymbol{k}) - E_F$ is the energy of the electron measured relative to the Fermi energy E_F, and the superscript 0 indicates the spin susceptibility with $\boldsymbol{q} = 0$. All of the other components vanish due to the symmetry of Fermi surface. The out-of-plane component χ_{zz}^0 is the so-called van Vleck susceptibility and originates from the virtual inter band transition. The in-plane component χ_{xx}^0 or χ_{yy}^0 contains both the intraband contribution (the Pauli susceptibility) and the interband contribution (the van Vleck susceptibility).

Numerical calculations of the spin susceptibilities of 2DEGs with the anisotropic Rashba SOC show two main features, as shown in Fig. 2. First, the spin susceptibilities are anisotropic, i.e., $\chi_{zz}^0 \neq \chi_{xx}^0$. Secondly, the spin susceptibilities have strong Fermi energy dependence. Note that the momentum cutoff k_c is used in our numerical calculations.

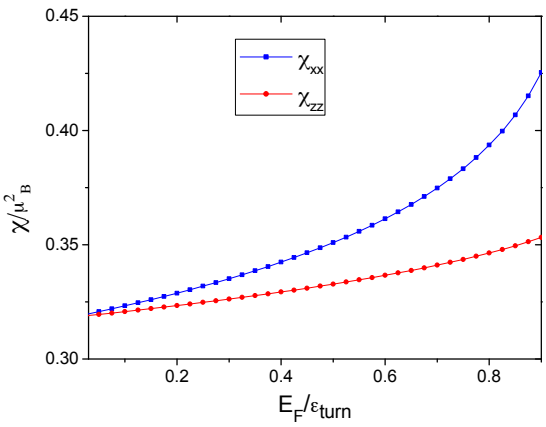

FIG. 2. (Color online) The spin susceptibility of 2DEG with the anisotropic Rashba SOC as function of the Fermi energy E_F in unit of $\varepsilon_{\rm turn}$ (measured from the bottom of the middle pair of bands). We set the dimensionless effective mass of the electron $m = 1$, the dimensionless Rashba SOC parameter $\beta = 0.01$ and the temperature T=5 K.

Previously the anisotropic spin susceptibility was also found using the k-linear Rashba model[38]. However, the spin susceptibility is anisotropic when only the lower Rashba spin-splitted band is occupied. As soon as both spin-splitted bands are occupied, the spin susceptibility becomes isotropic[39]. As such, the anisotropy only shows up in a small energy window. In contrast, the spin susceptibility in our model is always anisotropic (up to the turning point when the model is no longer valid)[40]. Therefore our result may provide an alternative explanation for the observed magnetic anisotropy[10,11].

Let us now turn to calculate the SHC of the 2DEG with the anisotropic Rashba SOC. The general spin conductivity tensor in the spin space is given as

$$\sigma_{\alpha x}^{\sigma_i} = \frac{\hbar}{2\pi L^2}\sum_{\boldsymbol{k}} {\rm Tr}\left[J_\alpha^{\sigma_i}\tilde{K}_x\right], \tag{16}$$

where $\tilde{K}_x \equiv UK_xU^\dagger$ is the vertex function in the spin space and $K_x = \tilde{G}^R J_x \tilde{G}^A$ is the vertex function in the eigenvectors space of $H_{\rm mid}(\boldsymbol{k})$. $\tilde{G}^R$ and $\tilde{G}^A$ are the retarded and advanced Green's function of 2DEG,

$$\tilde{G}_{\boldsymbol{k}s}^A(\epsilon) = \frac{1}{\epsilon - \varepsilon_{\boldsymbol{k}s} - i\eta}, \; \tilde{G}_{\boldsymbol{k}s}^R(\epsilon) = \frac{1}{\epsilon - \varepsilon_{\boldsymbol{k}s} + i\eta}, \tag{17}$$

where η is a positive infinitesimal. J_α stands for the velocity operator in the eigenvectors space and is given by $J_\alpha = U^\dagger j_\alpha U$ where $j_\alpha = ev_\alpha$ is the current operator of electron in the spin space and $v_\alpha = \partial H_{\rm mid}/\partial(\hbar k_\alpha)$ refers to the velocity operator with $\alpha = x, y$. The spin

current operators are represented by

$$J_{\alpha}^{\sigma_i} = \frac{\hbar}{4}\{v_{\alpha}, \sigma_i\}, \tag{18}$$

where $\{A, B\} \equiv AB + BA$ is an anti-commutator, and the 2×2 unitary transformation matrix is of the form

$$U = \frac{1}{\sqrt{2}} \begin{pmatrix} -i\varsigma_{\boldsymbol{k}} e^{-i\theta_{\boldsymbol{k}}} & i\varsigma_{\boldsymbol{k}} e^{-i\theta_{\boldsymbol{k}}} \\ 1 & 1 \end{pmatrix}. \tag{19}$$

After taking the trace over the spin degree of freedom, we have the nonzero component of the intrinsic SHC as

$$\sigma_{yx}^{\sigma_z} = \frac{eb\lambda\hbar^2}{16\pi^2} \int_0^{k_c} \frac{k^4 dk}{E_F - \hbar^2 k^2/2m} \int_0^{2\pi} \varsigma_{\boldsymbol{k}} \sin^2\theta_{\boldsymbol{k}} \times \cos 2\theta_{\boldsymbol{k}} [\delta(E_F - \varepsilon_{\boldsymbol{k}-}) - \delta(E_F - \varepsilon_{\boldsymbol{k}+})] d\theta_{\boldsymbol{k}}, \tag{20}$$

which indicates that a spin Hall current along the y direction and polarized in the z direction may exist when an external electric field is applied along the x direction. The symbols b and λ are defined as $b = \hbar/m$ and $\lambda = \beta\hbar^2$, respectively. In the weak anisotropy limit ($\beta \ll (2m\hbar k_F)^{-1}$), we keep the leading-order contribution to the intrinsic SHC and find

$$\sigma_{yx}^{\sigma_z} = -\frac{e}{8\pi}, \tag{21}$$

which is identical to that of the 2DEG with k-linear Rashba SOC[36] but is different from 2DEG with the k-cubed Rashba SOC[41,42]. The vanishment of the other components of the spin conductivity tensor is due to the symmetry of the Fermi surface.

Now we consider the impact of disorder on the SHC up to the vertex correction. It is more convenient to implement the calculation in the eigenvector space. We consider the randomly distributed, identical point defects that are spin independent: $V(\boldsymbol{r}) = \sigma_0 V_0 \sum_i \delta(\boldsymbol{r} - \boldsymbol{R}_i)$ and the matrix element can be expressed as

$$V_{\boldsymbol{k}\boldsymbol{k}'}^{ss'} = \frac{V_0}{2L^2} \sum_i e^{-i(\boldsymbol{k}-\boldsymbol{k}')\cdot\boldsymbol{R}_i} \left(1 + ss'\varsigma_{\boldsymbol{k}}\varsigma_{\boldsymbol{k}'} e^{-i(\theta_{\boldsymbol{k}'} - \theta_{\boldsymbol{k}})}\right), \tag{22}$$

where V_0 is the strength of defect potential and $\mathbf{R}_i$ is the position of the defect. The self-energy in the first order Born approximation can be written as

$$\begin{aligned} &\left\langle \langle \boldsymbol{k}s | VG_0V | \boldsymbol{k}'s' \rangle \right\rangle_{AV} \\ =&\frac{nV^2}{4L^2}\delta_{\boldsymbol{k}\boldsymbol{k}'} \sum_{\boldsymbol{k}_1 s_1} g_{\boldsymbol{k}_1 s_1} (1 + ss'\varsigma_{\boldsymbol{k}}\varsigma_{\boldsymbol{k}'}) \\ =&\delta_{s_1 s_2}\delta_{\boldsymbol{k}\boldsymbol{k}'} \frac{nV^2}{2L^2} \sum_{\boldsymbol{k}_1 s_1} g_{\boldsymbol{k}_1 s_1} = \delta_{\boldsymbol{k}\boldsymbol{k}'}\delta_{ss'}\Sigma_{\boldsymbol{k}s}, \end{aligned} \tag{23}$$

where $n = N/L^2$ is the density of impurities per unit area and $\langle\langle \cdots \rangle\rangle_{AV}$ denotes the ensemble averaging over the impurity distribution. We have introduced the relation of disorder-free Green's function: $\langle \boldsymbol{k}_1 s_1 | G_0 | \boldsymbol{k}_2 s_2 \rangle = \delta_{s_1 s_2}\delta_{\boldsymbol{k}_1\boldsymbol{k}_2} g_{\boldsymbol{k}_1 s_1}$. Thus the disordered Green's function turns out to be

$$\left\langle \langle \boldsymbol{k}s | G | \boldsymbol{k}'s' \rangle \right\rangle_{AV} = \frac{1}{g_{\boldsymbol{k}s}^{-1} - \Sigma_{\boldsymbol{k}s}} \delta_{ss'}\delta_{\boldsymbol{k}'\boldsymbol{k}} = \tilde{G}_{\boldsymbol{k}s}. \tag{24}$$

For the ladder diagram correction to the velocity operator, we have the following iterative equation

$$\tilde{v}_{s_1,s_2}^x(\boldsymbol{k}) = v_{s_1,s_2}^x(\boldsymbol{k}) + \sum_{\boldsymbol{k}'} \sum_{s_3,s_4} \left\langle \left\langle V_{\boldsymbol{k}\boldsymbol{k}'}^{s_1 s_3} V_{\boldsymbol{k}'\boldsymbol{k}}^{s_4 s_2} \right\rangle \right\rangle_{AV} \times \tilde{G}_{s_4}^R(\boldsymbol{k}') \tilde{G}_{s_3}^A(\boldsymbol{k}') \tilde{v}_{s_3,s_4}^x(\boldsymbol{k}'), \tag{25}$$

where $\tilde{v}^x$ is the corrected velocity operator, $s_{1,2,3,4} = \pm 1$.

It is difficult to solve analytically the above self-consistent equation due to the anisotropic dispersion. However, by considering the weak SOC limit, i.e., $\mathrm{Im}\Sigma_{k_F} \ll \beta\hbar^3 k_F^3 \ll \frac{\hbar^2 k_F^2}{2m}$, the equation can be approximately solved by keeping the leading order of β, where k_F is the Fermi wave vector and Σ_{k_F} is the self-energy.

After lengthy but straightforward calculations, we can find the corrected velocity operator (its derivation is presented in the Supplementary Materials[31])

$$\tilde{v}^x(\boldsymbol{k}) = v^x(\boldsymbol{k}) + \beta m E_F \sigma_y. \tag{26}$$

Following the similar procedure in Eq. (16), we can calculate the SHC with the vertex correction in the weak anisotropy limit and get

$$\left[\sigma_{yx}^{\sigma_z}\right]_{\mathrm{V}} = -\frac{e}{16\pi}. \tag{27}$$

It can be seen that in the weak anisotropy limit, the vertex correction reduces the magnitude of SHC by a factor of 2. In fact, this unique feature of SHC under the influence of disorder originates from the special form of Rashba SOC. Our result is qualitatively consistent with the fact that the term $\alpha k^2 (\boldsymbol{k} \times \boldsymbol{\sigma}) \cdot \hat{z}$ would result in a nonzero SHC even with the vertex correction[43]. On the other hand, the vertex correction of disorder can cause the intrinsic SHC of 2DEG with standard k-linear Rashba SOC to vanish identically[44], but does not affect the one with k-cubed Rashba SOC[45]. Hence, the distinct behaviors of SHC can be used to determine the nature of the Rashba SOC at LAO/STO interface.

In summary, we have developed an effective Hamiltonian of the 2DEG at the oxide interface LAO/STO and found a new anisotropic Rashba SOC. We have found that the static spin susceptibilities are anisotropic and dependent on the Fermi energy. We have also demonstrated that this new Rashba SOC possesses entirely different behavior for the SHC under disorder. Therefore, these unconventional spin responses can be used to determine the nature of Rashba SOC in experiments.

We are grateful to Matthew Daniels for a careful reading of the manuscript. This work is supported by AFOSR No. FA9550-12-1-0479 and No. FA9550-14-1-0277.

* jhzhou@andrew.cmu.edu
† wyshan@andrew.cmu.edu

[1] A. Ohtomo and H. Y. Hwang, Nature **427**, 423 (2004).
[2] H. Y. Hwang, Y. Iwasa, M. Kawasaki, B. Keimer, N. Nagaosa and Y. Tokura, Nature Materials **11**, 103 (2012).
[3] A. D. Caviglia, S. Gariglio, N. Reyren, D. Jaccard, T. Schneider, M. Gabay, S. Thiel, G. Hammerl, J. Mannhart, and J.-M. Triscone, Nature **456**, 624 (2008).
[4] C. Bell, S. Harashima, Y. Kozuka, M. Kim, B. G. Kim, Y. Hikita, and H. Y. Hwang, Phys. Rev. Lett. **103**, 226802 (2009).
[5] S. Thiel, G. Hammerl, A. Schmehl, C. W. Schneider and J. Mannhart, Science **313**, 1942–1945 (2006).
[6] Zoran S. Popović, Sashi Satpathy, and Richard M. Martin, Phys. Rev. Lett. **101**, 256801 (2008).
[7] J.-S. Lee, Y. W. Xie, H. K. Sato, C. Bell, Y. Hikita, H. Y. Hwang and C.-C. Kao, Nature Materials **12**, 703 (2013).
[8] N. Reyren, S. Thiel, A. D. Caviglia, L. Fitting Kourkoutis, G. Hammerl, C. Richter, C. W. Schneider, T. Kopp, A.-S. Retschi, D. Jaccard, M. Gabay, D. A. Muller, J.-M. Triscone, J. Mannhart, Science **317**, 1196 (2007).
[9] D. A. Dikin, M. Mehta, C. W. Bark, C. M. Folkman, C. B. Eom, and V. Chandrasekhar, Phys. Rev. Lett. **107**, 056802 (2011).
[10] L. Li, C. Richter, J. Mannhart, and R. C. Ashoori, Nature Phys. **7**, 762 (2011).
[11] J. A. Bert, B. Kalisky, C. Bell, M. Kim, Y. Hikita, H. Y. Hwang and K. A. Moler, Nature Phys. **7**, 767 (2011).
[12] Alexey Kalabukhov, Robert Gunnarsson, Johan Brjesson, Eva Olsson, Tord Claeson, and Dag Winkler, Phys. Rev. B 75, 121404 (2007).
[13] G. Herranz, M. Basletić, M. Bibes, C. Carrtro, E. Tafra, E. Jacquet, K. Bouzehouane, C. Deranlot, A. Hamzić, J.-M. Broto, A. Barthlmy, and A. Fert, Phys. Rev. Lett. **98**, 216803 (2007).
[14] D. R. Hamann, D. A. Muller, and H. Y. Hwang, Phys. Rev. B, **73**, 195403 (2006).
[15] S. Okamoto, A. J. Millis, and N. A. Spaldin, Phys. Rev. Lett. **97**, 056802 (2006).
[16] A. D. Caviglia, M. Gabay, S. Gariglio, N. Reyren, C. Cancellieri, and J.-M. Triscone, Phys. Rev. Lett. **104**, 126803 (2010).
[17] M. Ben Shalom, A. Ron, A. Palevski, and Y. Dagan, Phys. Rev. Lett. **105**, 206401 (2010).
[18] Y. A. Bychkov and E. I. Rashba, J. Phys. C **17**, 6039 (1984).
[19] K. Michaeli, A. C. Potter, and P. A. Lee, Phys. Rev. Lett. **108**, 117003 (2012).
[20] S. Banerjee, O. Erten and M. Randeria, Nature Phys. **9**, 626 (2013).
[21] X. P. Li, W. V. Liu, L. Balents, Phys. Rev. Lett. **112**, 067202 (2014).
[22] Sumilan Banerjee, James Rowland, Onur Erten, and Mohit Randeria, Phys. Rev. X **4**, 031045 (2014).
[23] M. S. Scheurer and J. Schmalian, Nat. Commun. **6**, 6005 (2015).
[24] Lorien X. Hayden, R. Raimondi, M. E. Flatt, and G. Vignale, Phys. Rev. B **88**, 075405 (2013).
[25] H. Nakamura, T. Koga, and T. Kimura, Phys. Rev. Lett. **108**, 206601 (2012).
[26] Younghyun Kim, Roman M. Lutchyn, and Chetan Nayak, Phys. Rev. B **87**, 245121 (2013).
[27] G. Khalsa, B. Lee, and A. H. MacDonald, Phys. Rev. B **88**, 041302 (2013).
[28] Z. Zhong, A. Tth, and K. Held, Phys. Rev. B **87**, 161102 (2013).
[29] L. W. van Heeringen, G. A. de Wijs, A. McCollam, J. C. Maan, and A. Fasolino, Phys. Rev. B **88**, 205140 (2013).
[30] R. Winkler, *Spin Orbit Coupling Effects in Two-Dimensional Electron and Hole Systems* (Springer, New York, 2003).
[31] Supplemental Material contains the derivation of the effective Hamiltonians with the specific expression of its parameters and the derivation of the corrected velocity operator.
[32] W. Meevasana, P. D. C. King, R. H. He, S.-K. Mo, M. Hashimoto, A. Tamai, P. Songsiriritthigul, F. Baumberger, and Z.-X. Shen, Nat. Mater. **10**, 114 (2011).
[33] The two branches of anisotropic Rashba SOC do not actually touch each other when higher-order correction is taken into account.
[34] C. Cancellieri, M. L. Reinle-Schmitt, M. Kobayashi, V. N. Strocov, P. R. Willmott, D. Fontaine, Ph. Ghosez, A. Filippetti, P. Delugas, and V. Fiorentini, Phys. Rev. B **89**, 121412(R) (2014).
[35] P. D. C. King, S. McKeown Walker, A. Tamai, A. de la Torre, T. Eknapakul, P. Buaphet, S.-K. Mo, W. Meevasana, M. S. Bahramy and F. Baumberger, Nature Communications **5**, 3414 (2014).
[36] J. Sinova, D. Culcer, Q. Niu, N. A. Sinitsyn, T. Jungwirth, and A. H. MacDonald, Phys. Rev. Lett. **92**, 126603 (2004).
[37] S. Murakami, N. Nagaosa, and S. C. Zhang, Science **301**, 1348 (2003).
[38] Mark H Fischer, Srinivas Raghu and Eun-Ah Kim, New J. Phys. **15**, 023022 (2013).
[39] R. A. Żak, D. L. Maslov, and D. Loss, Phys. Rev. B. **82**, 115415 (2010).
[40] The spin susceptibilities of 2DEG with k-cubed Rashba SOC have the same qualitative features as 2DEG with an anisotropic Rashba SOC but some quantitative differences.
[41] John Schliemann and Daniel Loss, Phys. Rev. B **71**, 085308 (2005).
[42] The spin Hall conductivity of 2DEG with k-cubed Rashba SOC takes the value of $\sigma_{\rm SH} = 3e/8\pi$ by the definition of spin current in Eq. (18).
[43] S. Murakami, Phys. Rev. B **69**, 241202 (2004).
[44] J. I. Inoue, G. E. W. Bauer, and L. W. Molenkamp, Phys. Rev. B **70**, 041303 (2004).
[45] B. Andrei Bernevig and Shou-Cheng Zhang, Phys. Rev. Lett. **95**, 016801 (2005).